Vibrational properties of the high-pressure Cmcm phase of ZnTe

J. Camacho,[1,2] K. Parlinski,[3] A. Cantarero,[2] and K. Syassen[1]

[1] *Max-Planck-Institut für Festkörperforschung, Heisenbergstraße 1, D-70569 Stuttgart, Germany*
[2] *Materials Science Institute, University of Valencia, P. O. Box 22085, E-46071 Valencia, Spain*
[3] *Institute of Nuclear Physics, ul. Radzikowskiego 152, 31-342 Cracow, Poland*

(Dated: December 18, 2003)

A lattice dynamical model based on *ab initio* methods has been developed for the common Cmcm-type orthorhombic high-pressure phase of binary semiconductors. It is applied to ZnTe. The model supplies the zone-center phonon frequencies which are compared to experimental Raman scattering results. The complete phonon dispersion relations and the one-phonon density of states of Cmcm-ZnTe are calculated. The phonon eigenvectors at the Γ−point of the Brillouin zone are given.

PACS numbers: 62.50.+p, 78.30.Fs, 63.20.Dj, 78.20.Bh

I. INTRODUCTION

Several tetrahedrally coordinated III-V and II-VI semiconductors adopt an orthorhombic crystal structure under pressure with space group Cmcm and Z=4 formula units per unit cell.[1,2] The structure can be viewed as a distorted variant of the rocksalt structure (see Fig. 1). The structure type, which we denote by its space group in the following, was first identified for ZnTe.[3] For this compound (and CdSe as well) the structural sequence under pressure is zincblende→cinnabar→Cmcm. The stability range of the Cmcm phase of ZnTe extends from 12 to about 85 GPa, where a new modification appears. In CdTe (as in other II-VI and III-V compounds) a rocksalt-type phase occurs *before* transformation to a Cmcm phase.[1,2]. Such differences in phase stability behavior have been correlated with the degree of ionicity.[4,5]

Given the low ionicity of ZnTe (compared to other II-VI compounds) and the relatively high atomic coordination of the Cmcm phase,[1] this modification can be expected to be metallic. In fact, at pressures higher than ∼12 GPa metallic-like transport properties are observed.[6] Furthermore, in near-infrared reflectivity measurements a Drude-like tail appears at the phase transition from semiconducting cinnabar to Cmcm.[7,8]

The first observation of the Cmca structure in ZnTe[3] and followup experimental studies of other binaries initiated quite a number of *ab initio* total energy calculations; most of the theoretical work is covered in a recent review.[2] Specifically for Cmcm-ZnTe, calculations were reported in Refs. 9–13. The obtained band structure of Ref. 11 is consistent with metallic behavior.

In contrast to experimental and theoretical phase stability, the lattice dynamical properties characteristic of the ubiquitous Cmcm-type structure are not well known. A few Raman data were reported for Cmcm-ZnTe,[14] but no detailed interpretation could be given in terms of a quantitative phonon model.

Here we report lattice dynamics calculations of Cmcm-ZnTe based on *ab initio* pseudopotentials which allow us to obtain the dynamical matrix. The method provides frequencies and eigenvectors in the complete Brillouin zone and thus, the phonon density of states. The calculated zone-center frequencies are compared to Raman data. Of the six Raman-active modes predicted by group theory four are observed experimentally. These are assigned on the basis of the calculated results.

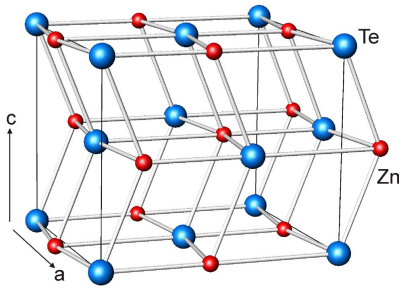

FIG. 1: The orthorhombic crystal structure of Cmcm-ZnTe. Experimental lattice parameters at 15.7 GPa are $a = 5.379(1)$ Å, $b = 5.971(1)$ Å and $c = 5.010(2)$ Å (Ref. 3). The Zn and Te atoms both occupy Wyckoff 4c sites with $y_{\mathrm{Zn}} = 0.640(1)$ and $y_{\mathrm{Te}} = 0.190(1)$. Note that the origin of the unit cell indicated in the figure is shifted in order to facilitate comparison with a NaCl-type structure.

II. CALCULATIONS

The primitive cell of the Cmcm structure contains two formula units. In terms of the lattice vectors of the orthorhombic Bravais lattice, a possible choice of primitive lattice vectors is $\boldsymbol{a}_1=(a/2,-b/2,0)$, $\boldsymbol{a}_2=(a/2,b/2,0)$, $\boldsymbol{a}_3=(0,0,c)$, $abc/2$ being the volume of the primitive unit cell. The reciprocal lattice vectors are $\boldsymbol{b}_1=(1/a,-1/b,0)$, $\boldsymbol{b}_2=(1/a,1/b,0)$, $\boldsymbol{b}_3=(0,0,1/c)$. The angle between $\boldsymbol{b}_1$ and $\boldsymbol{b}_2$ is 84°, i.e. the net is close to tetragonal, see Fig. 2.

A factor group analysis leads to 12 vibrational modes at the Γ-point:

$$\Gamma = 2\mathrm{A}_g + 2\mathrm{B}_{1g} + 2\mathrm{B}_{1u} + 2\mathrm{B}_{2u} + 2\mathrm{B}_{3g} + 2\mathrm{B}_{3u}\,.$$

The six *gerade* modes, $2\mathrm{A}_g$, $2\mathrm{B}_{1g}$ and $2\mathrm{B}_{3g}$, are Raman-active and three of the six *ungerade* modes, B_{1u}, B_{2u},

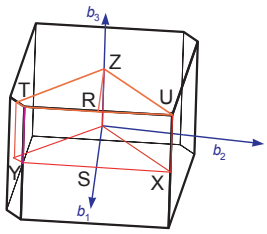

FIG. 2: Brillouin zone of the Cmcm structure. The basis vectors of the reciprocal lattice $\boldsymbol{b}_1$, $\boldsymbol{b}_2$, and $\boldsymbol{b}_3$ (see text) are indicated. Note the near right angle between $\boldsymbol{b}_1$ and $\boldsymbol{b}_2$.

and B_{3u}, are the acoustic ones. The remaining three are infrared-active modes. Thus, 12 phonon branches are expected for a general value of $\boldsymbol{q}$.

The vibrational properties of the Cmcm phase of ZnTe have been analyzed following *ab initio* methods. The calculations use the density functional theory (DFT) with the general gradient approximation (GGA) as implemented in the VASP package,[15,16] and with Vanderbilt-type ultrasoft pseudopotentials[17] provided with VASP. This package solves the generalized Kohn-Sham equations by an iterative matrix diagonalization based on the minimization of the norm of the residuum vector for each eigenstate and an optimized charge-density mixing routine. The pseudopotentials for the Zn and Te atoms are representing $d^{10}s^2$ and s^2p^4 electron configurations, respectively. A plane-wave basis set was used to expand the electronic wave functions at special k-points generated by a $6 \times 6 \times 6$ Monkhurst-Pack k-mesh.

We have used the crystallographic orthorhombic unit cell with 8 atoms to optimize the crystal structure at a pressure of 11.6 GPa. The resulting lattice parameters are $a = 5.4265$, $b = 6.0889$ and $c = 5.0009$ Å, the free positional parameters are $y_{\rm Zn} = 0.6289$ and $y_{\rm Te} = 0.1898$. The axial ratios and positions compare well with the experimental values given in Ref. 3. The calculated cell

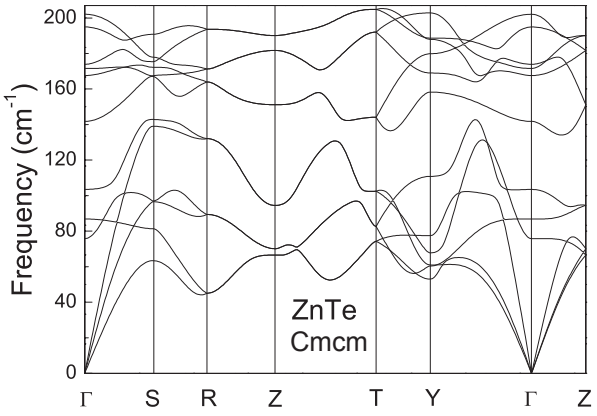

FIG. 3: Calculated phonon dispersion relations for the Cmcm phase of ZnTe for a cell volume of 165.2 Å^3 (12.3 GPa experimental pressure). The high-symmetry points of the Brillouin zone are labelled according to the standard notation.

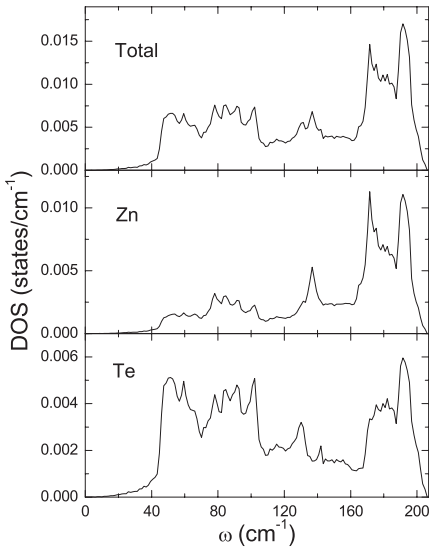

FIG. 4: Total (higher panel) and partial phonon density of states for Zn (medium panel) and Te (lower panel) atoms in Cmcm-ZnTe. Note that vertical scales are different for the different panels.

volume of 165.2 Å^3 ($V/V_0 = 0.725$, V_0 being the volume of the cubic phase at ambient conditions) corresponds to an experimental pressure of about 12.3 GPa (based on an interpolation of data given in Ref. 3).

The phonons were determined by a direct method[18,19] using an optimized supercell subjected to the symmetry of the Cmcm space group. A $2 \times 2 \times 2$ supercell with 64 atoms was constructed for that purpose, the special k-points were generated by a $3 \times 3 \times 3$ Monkhurst-Pack scheme, and the Hellmann-Feynman forces were computed for independent displacements required by the symmetry of the unit cell. The displacement amplitudes were 0.03 Å. Positive and nega-

TABLE I: Zone-center phonons of the Cmcm phase of ZnTe: Calculated optical mode frequencies at a cell volume of 165.2 Å^3 (experimental pressure 12.3 GPa), measured frequencies at 12.2 GPa, average linear pressure coefficients for the range 11–15 GPa, and corresponding mode Grüneisen parameters γ. The γ-values refer to an an estimated bulk modulus value of B=117 GPa at 12.3 GPa.

Mode	ω (cm^{-1})		$d\omega$/dP (cm^{-1}/GPa)	γ
	calc	expt		
B_{1g}	75.72	53(4)	0.93(10)	2.1(3)
B_{3g}	86.73	88(1)	2.0(4)	2.7(5)
A_g	103.40	97.9(2)	1.52(14)	1.9(2)
B_{1u}	141.76	–		
B_{3u}	168.12	–		
A_g	171.45	161.3(2)	1.90(6)	1.41(4)
B_{2u}	173.79	–		
B_{1g}	194.80	–		
B_{3g}	202.14	–		

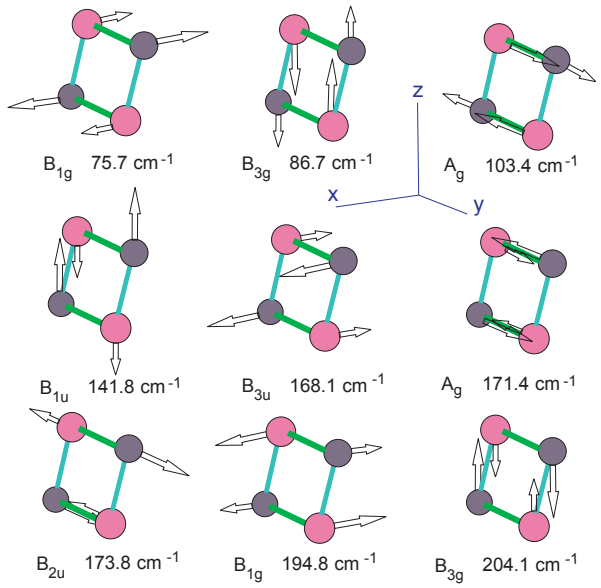

FIG. 5: Atom displacements for the zone-center vibrational modes of the Cmcm phase of ZnTe. The phonon frequencies calculated for a cell volume of 165.2 Å^3 (experimental pressure 12.3 GPa) are also given.

tive atomic displacements along x, y and z directions were used. These displacement configurations generate 2304 components of Hellmann-Feynman forces. Using the program PHONON,[20] which incorporates 50 force constant matrices, with 288 independent parameters, the force constant parameters are fitted to the Hellmann-Feynman forces by the singular value decomposition algorithm, which simultaneously provides the least-square solution. Independent of the range of interaction, the direct method gives exact phonon frequencies at wave vectors commensurate with the supercell size, provided the supercell shape guarantees the complete list of neighbors of each coordination shell such that the dynamical matrix conserves its symmetry. The structures considered here satisfy this condition. For the studied Cmcm structure the exact phonon frequencies are obtained at all high-symmetry points (Γ, Y, Z, T, S, R) of the BZ (Fig. 2), and a few others in between. In ZnTe the values of the force constants cease out with distance by more than two orders of magnitude, therefore, the phonon branches should be correctly reproduced.

Since we have calculated the dynamical matrix, our approach provides the complete phonon dispersion relations. They are shown in Fig. 3 along the high-symmetry directions Γ–S–R–Z–T–Y–Γ – Z, calculated at 11.6 GPa. There are 12 phonon branches (four atoms in the primitive cell), all single degenerate, except the high-symmetry lines R–Z and Z–T along which all branches are doubly degenerate. **It should be noted that the calculations were performed by assuming that the effective charge is screened out due to the metallic nature of Cmcm-ZnTe.**

Figure 4 shows the one-phonon density of states (DOS). The total DOS as well as partial DOS corresponding to Zn and Te are given. As expected, the contribution of Te movements dominates at lower frequency, since Te is heavier than Zn. Different from the DOS of the zincblende phase,[14,21] no gap shows up in the DOS of Cmca.

The calculated phonon frequencies at the Γ–point are listed in the first column of Table I. The eigenvectors corresponding to these modes are shown in Fig. 5. Only the independent atoms (two formula units) are shown in the figure. All atoms are at $x = 0.5$, Zn_1 and Te_1 at $z = 0.25$ and Zn_2 and Te_2 at $z = 0.75$. The atomic movement of the modes is along x, y or z. The lowest-energy B_{1g} mode is a bending mode, where the atomic movement **fold the vertical and horizontal plane around the 90 degrees equilibrium position** and thus it is expected to have the lowest frequency. The next mode, B_{3g}, is a combination of stretching and bending. The first A_g mode is a kind of torsional mode, where the distorted rhombus is twisted by the atomic movement. The other A_g mode is the only pure stretching mode. The remaining *gerade* modes as well as the three infrared-active *ungerade* ones involve combinations of stretching and bending.

III. COMPARISON WITH EXPERIMENT

Raman spectra of the Cmcm phase of ZnTe are displayed in Fig. 6. The description of the experiment can be found elsewhere.[14] Although the Cmcm phase of ZnTe

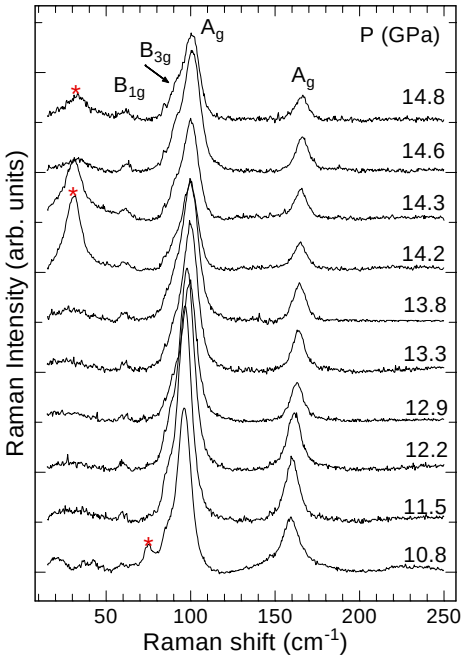

FIG. 6: Raman spectra of the Cmcm phase of ZnTe. Spectra from 14.2 GPa upwards are measured on upstroke, those at lower pressure on downstroke.

has a metallic character, the presence of free carriers does not preclude the detection of phonon Raman signals.

In Fig. 6, the three spectra at 14.2, 14.3 and 14.8 GPa were recorded for increasing pressure, whereas the remaining spectra were obtained with releasing pressure. Some of the upstroke spectra still show Raman modes belonging to the cinnabar phase; these are marked by stars to distinguish them from the Raman modes of the Cmcm phase. The cinnabar modes are not present when the pressure is released. For increasing pressure, the Cmcm phase of ZnTe was first observed near 13.7 GPa, on downstroke it is detected down to at least 10.8 GPa.

In the Raman spectra, only four of the six expected Raman modes are observed. The Raman frequencies measured at 12.2 GPa are given in Table I. From a comparison with the calculated frequencies, the two main peaks in the spectra are the two A_g modes. The B_{1g} mode shows as a rather weak feature but it is clearly observed in all spectra. The B_{3g} mode appears as a shoulder at the lower frequency tail of the A_g feature. The higher frequency B_{1g} and B_{3g} modes do not show up in the experimental spectra.

In Table I we list the dependence of the experimental phonon frequencies on pressure in the range from 10.8 to 16.0 GPa and the Grüneisen parameters of the observed Raman modes. The Grüneisen parameters are comparable to those of the LO and TO modes in the zincblende structure of ZnTe.[22] The value of the Grüneisen parameter of the B_{3g} mode is an exception, but its larger value compared to the rest of modes can probably be attributed to the inaccuracy in the determination of the mode frequency at different pressures (cf. Fig. 6).

IV. CONCLUSIONS

We have studied the vibrational properties of the Cmcm high-pressure phase of ZnTe by means of first-principle calculations with the aim of interpreting the Raman spectra of this high-pressure phase. The observed Raman features can be assigned on the basis of the phonon frequency calculations. The phonon dispersion curves along several high symmetry directions of the Brillouin zone have been obtained. The total and partial phonon densities of states are given as well. The results obtained here could be useful for interpreting Raman spectroscopic data of high-pressure Cmca phases of other binary semiconductors.

Acknowledgments

J. C. acknowledges financial support from Max-Planck-Gesellschaft and Deutscher Akademischer Austauschdienst (DAAD). This work was also partially supported by the State Committee of Scientific Research (KBN), grant No 5 PO3B 069 20.

[1] R. J. Nelmes and M. I. McMahon, in *High pressure in semiconductor physics*, edited by W. Paul and T. Suski, (Academic, New York 1998), p. 145; Vol. 54 of *Semiconductors and Semimetals*.
[2] A. Mujica, A. Rubio, A. Muñoz, and R. J. Needs, Rev. Mod. Phys. **75**, 833 (2003).
[3] R. J. Nelmes, M. I. McMahon, N. G. Wright, and D. R. Allan, Phys. Rev. Lett. **73**, 1805 (1994).
[4] V. Ozolins and A. Zunger, Phys. Rev. Lett. **82**, 767 (1999).
[5] A. Zunger, K. Kim, and V. Ozolins, phys. stat. sol (b) **223**, 369 (2001).
[6] A. Ohtani, M. Motobayashi, and A. Onodera, Phys. Lett. **75A**, 435 (1980).
[7] A. R. Goñi and K. Syassen, in *High pressure in semiconductor physics*, edited by W. Paul and T. Suski, (Academic, New York 1998), p. 248; Vol. 54 of *Semiconductors and Semimetals*.
[8] M. Kobayashi, Phys. Stat. Sol. (b) 223, 55 (2001).
[9] G-D. Lee and J. Ihm, Phys. Rev. B **53**, R7622 (1996).
[10] M. Côté, O. Zakhharov, A. Rubio, and M. L. Cohen, Phys. Rev. B **55**, 13025 (1997).
[11] G-D. Lee, C. Hwang, M. H. Lee, and J. Ihm, J. Phys.: Condens. Matter **9**, 6619 (1997). The band structure for Cmcm-ZnTe shown in this work is calculated for a non-primitive cell.
[12] N. E. Christensen, D. L. Novikov, R. E. Alonso, and C. O Rodriguez, phys. stat. sol. (b) **211**, 5 (1999).
[13] R. Franco, P. Mori-Sanchez, J. M. Recio, and R. Pandey, Phys. Rev. B **68**, 195208 (2003).
[14] J. Camacho, I. Loa, A. Cantarero, and K. Syassen, J. Phys.: Condens. Mat. **14**, 739 (2002); High Pressure Research **22**, 309 (2002).
[15] G. Kresse and J. Furthmüller, Software VASP, Vienna (1999); Comp.Mat.Science, **6**, 15 (1996); Phys.Rev. B **54**, 11169 (1996).
[16] G. Kresse and J. Hafner, Phys.Rev. B **47**, 558 (1993); *ibid* **49**, 14 251 (1994).
[17] D. Vanderbilt, Phys. Rev. B **41**, 7892 (1990).
[18] K. Parlinski, Z. Q. Li, and Y. Kawazoe, Phys. Rev. Lett. **78**, 4063 (1997).
[19] K. Parlinski, Am. Inst. Phys., Conference Proceedings 479, *Neutrons and numerical methods* N_2M, eds. M. R. Johnson, G. J. Kearley and H. G. Büttner, p.121 (1999).
[20] K. Parlinski, Software PHONON (2001).
[21] D. N. Talwar, M. Vandevyver, K. Kunc, and M. Zigone, Phys. Rev. B **24**, 741 (1981).
[22] B. A. Weinstein in *Procceedings of the* 13^{th} *Int. Conf. on the Physics of Semiconductors*, edited by F. G. Fumi, p. 326, Rome (1976); B. A. Weinstein, Solid State Commun. **24**, 595 (1977).